Investigation of Analogy between Boiling and Hydrogen Evolving System in Nucleate Bubble Regime

Hae-Kyun Park and Bum-Jin Chung*
Department of Nuclear Engineering, Kyung Hee University
#1732 Deogyeong-daero, Giheung-gu, Yongin-si, Gyeonggi-do, 17104, Korea
**Corresponding author: bjchung@khu.ac.kr*

1. Introduction

Operating a heat transfer device in boiling mode is preferable due to the high heat transfer rate compared to the single-phase heat transfer. Therefore, nucleate boiling has raised wide research interests worldwidely [1]. Also in nuclear areas, there have been numerous efforts to investigate the nucleate boiling, since all the nuclear power plants have steam generator [2]. However, the boiling experiments were not performed sufficiently due to the high power density, extreme thermal conditions, measurement difficulties, etc.

The present study aimed at simulating the saturated nucleate pool boiling phenomenon using Hydrogen Evolving System (HES). The reduction of hydrogen ions by electrochemical process substituted the vaporization process in the boiling system. The basic idea is that the hydrodynamic behavior of the both systems should be analogous. And our research group previously performed the related studies [3,4]. 1.5 M of sulfuric-acid (H_2SO_4) solution was used as working fluid and some bubble parameters such as nucleation site density (N_a), bubble departure diameter (D_b) and bubble frequency (f) were measured using thin wire and vertical disk plate as cathode surface, which simulated heating surface.

2. Theoretical Backgrounds

2.1 Nucleation site density

Gaertner and Westwater [5] observed that N_a increased with the heat flux as expressed in Eq. (1)

$$N_a \sim q''^{2.1}. \tag{1}$$

Paul and Abdel-Khalik [6] measured N_a using platinum wire and water at saturated condition. The individual bubble sites were counted at each heat flux step using high-speed camera. The results were fitted as

$$N_a = 1.207q'' - 1.574\times10^{-2}. \tag{2}$$

Yeom et al. [7] examined the influence of nanoparticle surface on the N_a using zirconium wire and water at saturated condition. The N_a was counted at each heat flux value up to the CHF. The N_a showed peak value before the CHF point, irrespective of the surface conditions.

Therefore, the N_a increases as the heat flux increases generally.

2.2 Bubble departure diameter

Fritz [8] developed the correlation, Eq. (3) to predict D_b introducing using contact angle of the bubble. Cole [9] developed the correlation using Ja, Eq. (4).

$$Bo_d^{0.5} = 0.0208\theta. \tag{3}$$

$$Bo_d^{0.5} = 0.04Ja,$$
$$\text{where } Bo_d = g\Delta\rho D_b^2/\sigma \text{ and } Ja = C_p\Delta T/h_{fg}. \tag{4}$$

Paul and Abdel-Khalik [6] and Yeom et al. [7] measured the D_b with respect to the heat flux with the identical apparatus measuring the N_a. Paul and Abdel-Khalik [6] found linear relationship between D_b and the heat flux. The D_b was also measured for individual bubble. However, Yeom et al. [7] reported that the bubble departure volume, which is proportional to the third power of the diameter, increased exponentially according to the heat flux up to the CHF point irrespective of the surface condition.

2.3 Bubble frequency

The liquid inertia carries the bubble away from the heating surface [10]. The time interval t_d is required for bubble to detach from the surface. Then the bulk liquid rushes after the bubble detachment and the time interval t_w is required for a subsequent nucleation [11]. Thus, bubble frequency can be expressed by

$$f = \frac{1}{t_w + t_d}. \tag{5}$$

Paul and Abdel-Khalik [6] calculated f based on the D_b data using frequency distribution function and obtained a linear relationship according to the heat flux. Yeom et al. [7] measured f by counting image frames for t_w and t_d and defined f as function of the heat flux up to the CHF. A peak was measured irrespective of the surface condition due to the bubble coalescence at a certain high heat flux condition.

3. Experimental setup

3.1 Test apparatus and electric circuit

Figure 1 shows the experimental apparatus and electric circuit. Two geometrical types of cathode were employed: 0.2 mm thick horizontal copper wire and vertical copper disk of 40 mm diameter. Three bubble parameters, N_a, D_b and f were measured using high speed camera with wire cathode at high current density. And in order to observe increased N_a at low current density, vertical disk cathode was employed. The cathode and the anode were located in the glass container filled with the aqueous solution of sulfuric acid (H_2SO_4) of 1.5 M at atmospheric pressure and room temperature, 294 K. The high-speed camera recorded the hydrogen bubbles at the cathode surface. The electric current was controlled using the power supply (N8952A, Keysight).

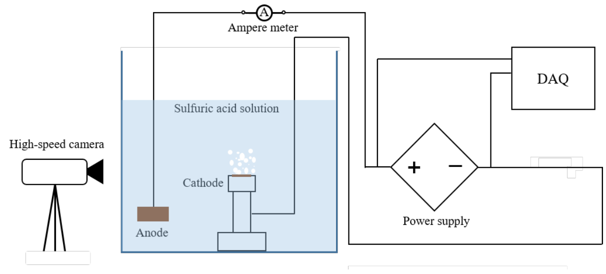

Fig. 1. Experimental apparatus and test section.

3.2 Test matrix

Table I sorted current density range. Low and high current densities were applied using vertical and horizontal cathode, respectively.

Table I: Range of current density for experiments

Current density scale (Cathode geometry)	**Current density range (A/m^2)**
Low current density (Vertical disk)	4.1–49.3
High current density (Horizontal wire)	3,900–94,700

4. Results and discussion

4.1. Nucleation site density

Figure 2 shows nucleation sites of the present hydrogen evolving system with respect to the current density at vertical disk within low current density range. The nucleation sites were randomly distributed on the cathode surface. The N_a increased as the current density increased, which is similar trend to the boiling system. However, it is difficult to quantify the N_a at the present system due to the numerous bubble sites.

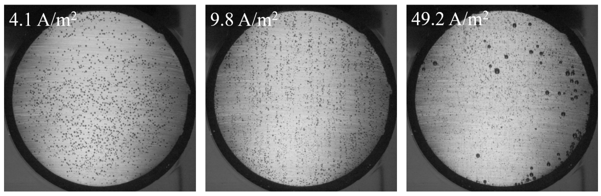

Fig. 2. Hydrogen bubble behaviors on the cylindrical ribbon.

Figure 3 compares the N_a between the boiling system and the present hydrogen evolving system at high current density range. Yeom et al. [7] measured the N_a up to the CHF point. They observed a peak value due to the bubble coalescence. Paul and Abdel-Khalik [6] also reported the similar trend. However, as they only measured the isolated bubble site at low heat flux, they could not observe the peak. Meanwhile in the present work, the bubble departure sites were measured as the N_a could not be measured due to the vigorous bubble coalescence at the high current density range. They decreased exponentially as the current density increased. Therefore, the N_a behavior and bubble departure site density in the present work are similar to that of the boiling system.

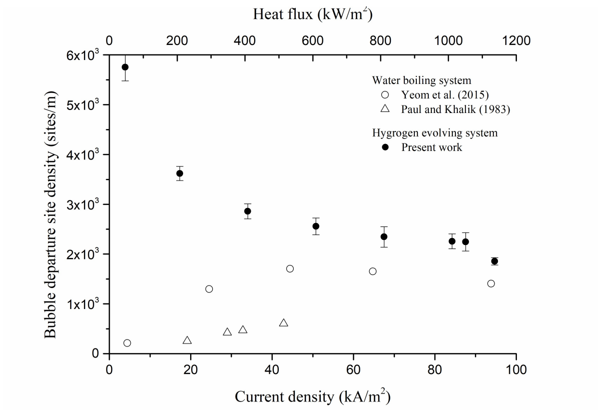

Fig. 3. Bubble departure site density of the boiling and the hydrogen evolving system.

4.2. Bubble departure diameter

Figure 5 shows the D_b of the boiling and the present hydrogen evolving system. Yeom et al. [7] and Paul and Abdel-Khalik [6] found the D_b increased as the heat flux increased. Similarly, the D_b of the present hydrogen evolving system increased as the current density increased as shown in Fig. 6. It is because of the vigorous bubble coalescence at the high heat flux and current density regime, which is predominated by the hydrodynamic phenomenon. However, the D_b in the hydrogen evolving system was smaller around 10% than that of the boiling system. Vogt et al. [12] insisted that the cell potential affects the wettability of the surface.

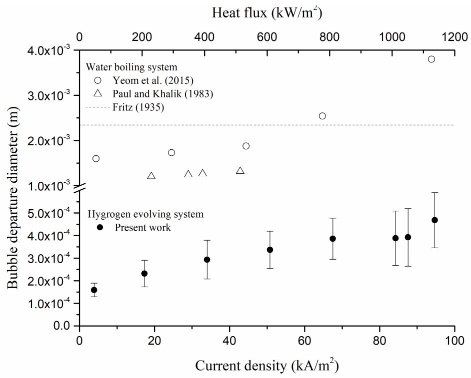

Fig. 5. Bubble departure diameter of the boiling and the hydrogen evolving system.

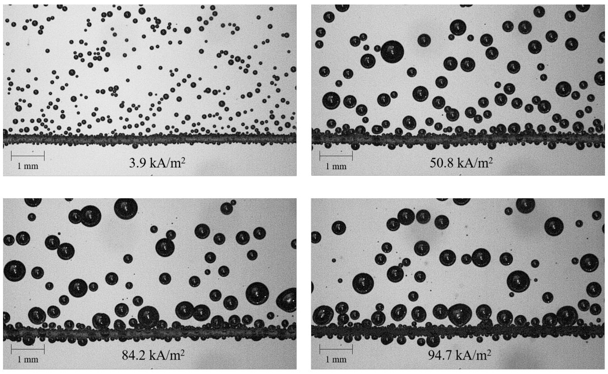

Fig. 6. Hydrogen bubble behaviors on the cylindrical ribbon.

4.3. Bubble frequency

Figure 7 represents the f of the boiling and hydrogen evolving system. In the boiling system, Paul and Abdel-Khalik [6] calculated the f based on the D_b and frequency distribution function. It showed the linear relationship with the heat flux. Also Yeom et al. [7] measured a peak value of f with respect to the heat flux due to the coalescence of the bubbles at the surface. The similar tendency of the f was measured in the hydrogen evolving system having a peak value with respect to the current density. Moreover, the absolute values of the f in the present work and Yeom et al. [7] were similar. It can be deduced that the existence of the peak value would be affected by the vigorous bubble interaction near the surface, similar to the boiling system. And thus it implies the hydrodynamic similarity between the two systems.

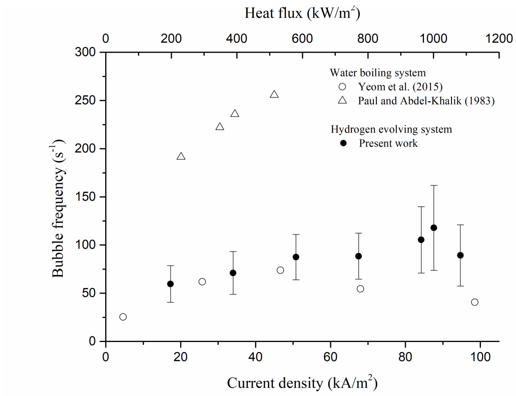

Fig. 7. Bubble frequency of the boiling and the hydrogen evolving system.

5. Conclusions

Saturated nucleate pool boiling phenomenon was simulated by the hydrogen evolving system using 1.5 M of sulfuric-acid solution and copper electrodes. The nucleation site density, the bubble departure diameter and the bubble frequency were measured by taking photographic image using high-speed camera. The similarities and the differences of the bubble behaviors between the hydrogen evolving and boiling system were discussed.

The nucleation site density according to the current density showed similar trend at the low heat flux and current density, since both the hydrogen and bubble generation mechanisms are dominated by the heterogeneous nucleation. The nucleation sites were increased as the heat flux or current density increased. However at the high heat flux and current density, the coalescence of bubbles reduced the bubble departure sites in both systems.

The tendency of the bubble departure diameter was similar between the two systems, meanwhile the diameters of the hydrogen bubble are small, around 10% of the vapor bubbles. The bubble frequency of the two systems were also similar, which showed peak values.

It is concluded that there is a certain analogous phenomenon between the boiling and the hydrogen evolving system in the hydrodynamic perspectives. The authors expect that the present work may contribute to establish the analogy research between the hydrogen evolving and the boiling system. However, the further investigation should be performed to establish improved analogy concept regarding the cell potential affecting the surface wettability and the surface tension.

Acknowledgement

This study was sponsored by the Ministry of Science and ICT and was supported by Nuclear Research & Development program grant funded by the National

Research Foundation (NRF) (Grant code: 2017M2A8A4015283).

REFERENCES

[1] H. Chen, G. Chen, X. Zou, Y. Yao, M. Gong, Experimental investigations on bubble departure diameter and frequency of methane saturated nucleate pool boiling at four different pressures, International Journal of Heat and Mass Transfer, Vol.112, pp.662-675, 2017.

[2] N. E. Todreas, M. S. Kazimi, Nuclear systems, Vol.1, second edition, CRC Press, New York, p.697, 2012.

[3] H. K. Park, B. J. Chung, Simulation of critical heat flux phenomenon using a non-heating hydrogen evolving system, Frontiers in Energy Research, Vol.7, Article 139, 2019.

[4] S. M. Ohk, H. K. Park, B. J. Chung, CHF experiments on the influence of inclination and gap size, International Journal of Heat and Mass Transfer, Vol.132, pp.929-938, 2019.

[5] R. F. Gaertner, J. W. Westwater, Population of active sites in nucleate boiling heat transfer, Chemical Engineering Progress Symposium Series, Vol.59, pp.39-48, 1960.

[6] D. D. Paul, S. I. Abdel-Khalik, A statistical analysis of saturated nucleate boiling along a heated wire, International Journal of Heat and Mass Transfer, Vol.26, pp.509-519, 1983.

[7] H. Yeom, K. Sridharan, M. L. Corradini, Bubble dynamics in pool boiling on nanoparticle-coated surfaces, Heat Transfer Engineering, Vol.36, pp.1027-1027, 2015.

[8] W. Fritz, Berechnung des Maximalvolumens von Dampfblasen, Physikalische Zeitschrift, Vol.36, pp.379-384, 1935.

[9] R. Cole, Bubble frequencies and departure volumes at subatmospheric pressures, AIChE. Journal, Vol.13, pp.779-783, 1967.

[10] P. Griffith, Bubble growth rates in boiling, Journal of Heat Transfer, Vol.80, pp.721-727, 1958.

[11] L. S. Tong, Y. S. Tang, Boiling heat transfer and two-phase flow, second ed., CRC Press, New York, 1997.

[12] H. Vogt, Ö. Aras, R. J. Balzer, The limits of the analogy between boiling and gas evolution at electrodes, International Journal of Heat and Mass Transfer, Vol.47, pp.787-795, 2004.